Intern report ; IR 2007-02

Site specific hazard estimates for the NUON energy plant in the Eemshaven

T. van Eck, F.H. Goutbeek and B. Dost

De Bilt, 2007

KNMI internal report = intern rapport; IR 2007-02

De Bilt, 2007

PO Box 201
3730 AE De Bilt
Wilhelminalaan 10
De Bilt
The Netherlands
http://www.knmi.nl
Telephone +31(0)30-220 69 11
Telefax +31(0)30-221 04 07

Authors: Eck, T. van
Goutbeek, F.H.
Dost, B.

Site specific hazard estimates for the NUON energy plant in the Eemshaven

T. van Eck, F.H. Goutbeek, B. Dost

De Bilt, March 2007

Contents

1. Introduction

NUON Energy Sourcing is planning to build a new energy plant in the Eemshaven in the north-eastern part of the Netherlands (figure 1). This plant will be situated on top of the Groningen-gas-reservoir, which is being exploited since 1963 causing small induced earthquakes. In order to be able to formulate appropriate building requirements NUON Energy Sourcing requested estimates of expected ground accelerations due to earthquakes in this area The KNMI has, since 1991, been recording almost 300 small earthquakes occurring in or close to the Groningen gas reservoir at about 3 kilometres depth. The magnitudes (M_L) of these events ranged from -0.2 to 3.5 and the depth of the earthquakes coincides with faults at the upper boundary of the gas-reservoir, the base of the Zechstein formation (see figure 2).

Figure 1. The Eemshaven with in red the location of the energy plant. (Source: NUON)

In van Eck et al. (2006) we show in a probability hazard analysis that Peak Ground Accelerations (PGA) estimates for the Eemshaven may range from 0.15 g to 0.25 g with associated annual probabilities of exceedance of 0.1 and 0.01 respectively. However, as described in the same paper, large uncertainties are associated with these estimates.

The purpose of this study is to provide NUON and TNO Bouw estimated site specific digital acceleration time series due to earthquakes in this area. Specifically, we estimated the expected accelerations for the largest possible earthquake at various distances with a low probability of occurrence and smaller earthquakes with a relatively high probability of occurrence and close to the plant.

In this report we present relevant observed and estimated accelerations, the methodology how we obtained the estimated accelerations, the maximum magnitude and the return period. We further present considerations about the uncertainties, specifically the source radiation pattern.

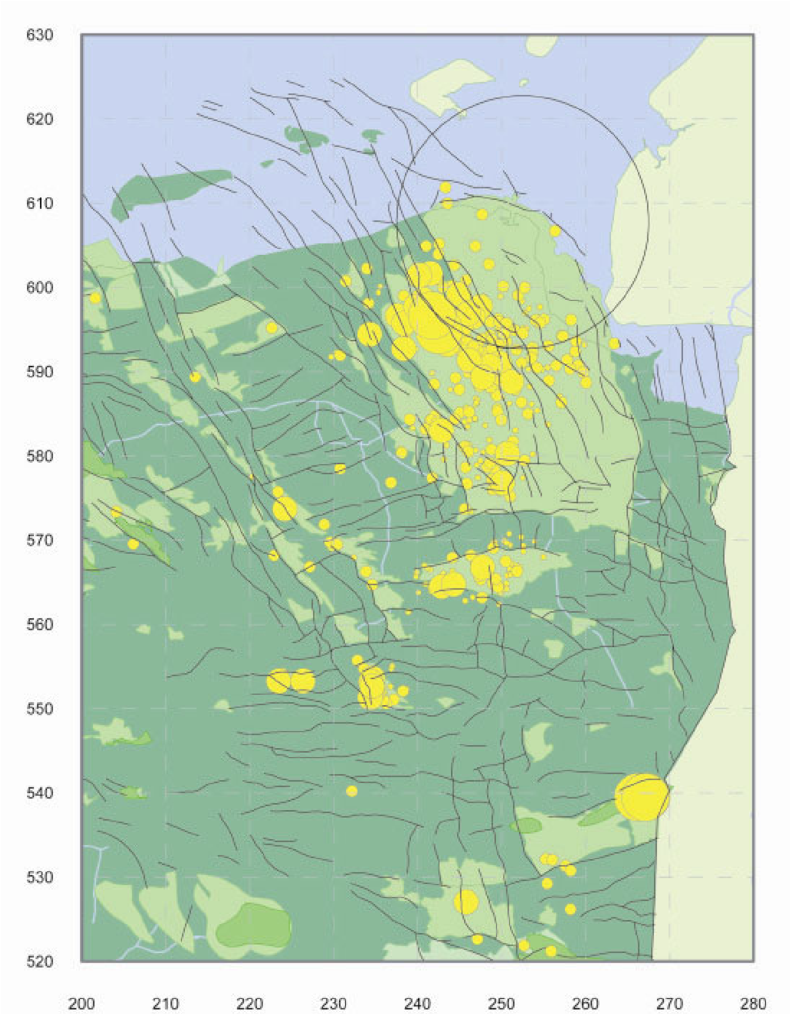

Figure 2. Observed seismicity in the Dutch provinces Groningen and Drenthe from 1986 to present (source KNMI, see also van Eck et 2006). The yellow dots of different sizes represent induced earthquakes of different magnitudes, the light green areas are known gas reservoirs and the dark gray lines are the faults at the base of the Zechstein formation at about 3 kilometres depth (source TNO). The northwest-southeast trending faults in the central part of the Groningen gas reservoir have hitherto proven to be most active. In this study we concentrate our interest on the seismicity within the large grey circle around the Eemshaven.

2. Seismicity characteristics

The observed seismicity up to February 2007 is shown in figure 2. The area around the northwest-southeast trending faults in the central part of the Groningen gas reservoir has up to now proven to be the most seismic active.
We assume that the seismicity will be equally distributed within the total gas field. This is a conservative estimate as currently we have seen much lower seismicity in the vicinity of the plant (figure 2).

Following this assumption we may estimate the seismicity rate and magnitude-frequency distribution for the area around the NUON energy plant. The seismicity that has an impact on the NUON energy plant may occur within a radius of about 15 km and the corresponding magnitude-frequency relation (lower curve in figure 3) indicates the return period for earthquakes of magnitude M or larger. For comparison we also show the magnitude-frequency relation for all observed induced seismicity in the Northern part of the Netherlands up to February 2007 (see also van Eck et al., 2006 for more details).

Unless the rate of the gas exploitation from the gas reservoir below the area around the NUON energy plant would change significantly we do not expect significant changes in the seismicity rate.

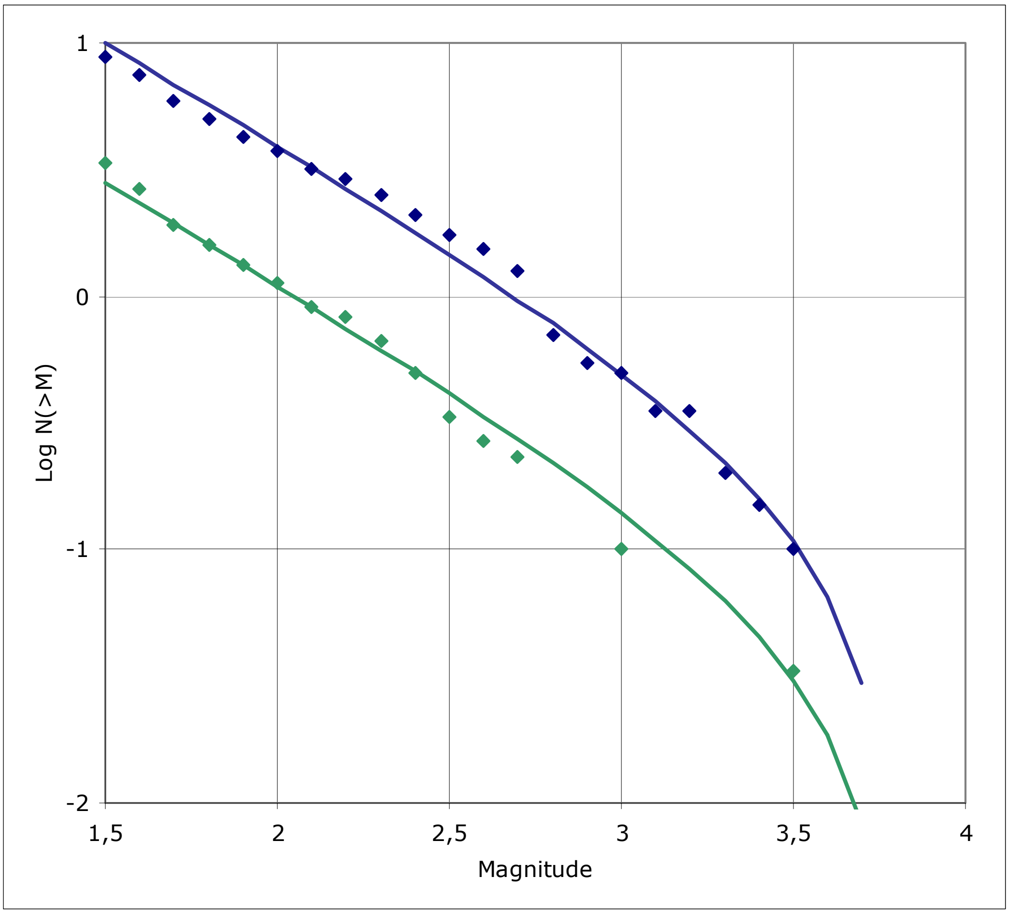

Figure 3. Annual cumulative frequency-magnitude relation for all events in the Northern part of the Netherlands and the northern part of the Groningen-gasfield (green curve). The observed data are represented in dots, the best fit curves are represented by the lines.

3. Estimating the maximum magnitude and its probability of occurrence

The approach chosen to estimate the probability of occurrence of relatively large induced earthquakes, with a very low probability, requires a different approach than is used for natural earthquakes. Natural earthquakes are driven by a stress build-up process in geologic time scale. For pragmatic hazard purposes this stress build-up is considered stationary.

For induced earthquakes the stress build-up is clearly time limited, i.e. not stationary, and we have good reasons to believe that the exploitation is not triggering tectonic scale earthquakes (van Eck et al., 2006). In the specific case of gas-exploitation-induced earthquakes in the Northern part of the Netherlands the stress build-up will stop once the reservoirs are emptied. This will most probably happen within the next 100 years, but depends of course on the exploitation policies.

Our approach to find a probably acceleration time series due to a large earthquake with a low probability of occurrence is, instead, to estimate the maximum probable earthquake that can occur, and associate with this earthquake an appropriate probable acceleration time series.

In earlier studies a number of approaches have been used to estimate the maximum probable earthquake:

- A mechanical model approach (Logan et al., 1997; De Crook et al., 1998) in which we model the largest possible earthquake from the maximum possible effective rupture surface area. Here we assume that the stress variations due to gas exploitation have maximum effect along a pre-existing fault within or at the border of a gas-field. Logan et al. (1997) arrived at an M_{max} estimate of M = 3.8.
- A synthetic seismicity approach (De Crook et al., 1998; Van Eck et al., 2006) in which we simulate a large number of seismicity scenarios constrained by the observed seismicity during approximately 20 years. In Van Eck et al. (2006) we obtained an M_{max} estimate of 3.9 based on the mean plus one standard deviation.

Consequently, based on a larger set of observations in the second approach, a good estimate of the maximum probable earthquake is M_L = 3.9. For simplicity we have chosen in this study to consider a M_L = 4.0 earthquake for modelling the largest probably acceleration time series. Its associated probability of occurrence is difficult to specify. Following the magnitude-frequency model as indicated in figure 3 it is definitively less than 1‰. Efforts to be more precise are unrealistic as this can only be based on speculations and/or unfounded extrapolations.

On the other hand for the area around the NUON facility we are fairly confident using figure 3 that earthquakes with $M_L \geq 2.3$ may occur with an annual probability of around 0.6 and earthquakes with $M_L \geq 3.0$ with an annual probability of around 0.1.

4. Estimated ground accelerations

4.1 Methodology

The estimated accelerations for the specified site are based on observed accelerations due to induced seismicity in the North of the Netherlands. The underlying assumption is that a possible acceleration shaking the prospective NUON plant would in quality be similar to those observed accelerations. We believe this assumption to be well founded as the expected mechanism of earthquakes causing such accelerations are expected to be similar and the earth structure underlying the Eemshaven does not differ significantly from those at other places in the Northern part of the Netherlands.

For the maximum probable earthquake we use a Green's function approach in which an observed acceleration is used to characterize the wave propagation effect on the earthquake signal. Essentially we applied an appropriate scaling procedure assuming self-similarity of the earthquake source processes involved, i.e. simple magnitude and size scaling, and assuming that the source function can be modelled by a Brune's model or ω^2 model (Aki and Richards, 1980).

Consequently, we selected a number of appropriate observed accelerations (Table 1) and computed for the maximum probable earthquake the estimated accelerations following the outlined Green's function approach for a number of magnitudes and distances.

The estimated site-specific accelerations are associated with an earthquake and its probability of occurrence. The argumentation for our selection of the earthquake size and its associated probabilities is given in the previous chapter.

Table 1a. Observed ground accelerations used for modelling the M_L = 4.0 acceleration records

Figures	Event date	Magnitude	Station	Delta (km)	Comments
Appendix A1, A2, A3	2006-08-08	3.5	Middelstum	3	Used in modelling the M_L=4.0 accelerations
			‘t Zand 2	4	
			‘t Zand 1	6	
			Hoeksmeer	9	

Table 1b. Observed ground accelerations used for modelling the M_L = 3.5 acceleration records

Figures	Event date	Magnitude	Station	Delta (km)	Comments
Figure 4	2007-01-26	2.5	‘t Zand 1	1	
			Westeremden	2	

Table 1c. Observed ground accelerations as samples of accelerations due to small near site earthquakes

Figures	Event date	Magnitude	Station	Delta (km)	Comments
Appendix A4, A5 and A6	2006-03-21	2.4	Hoeksmeer	2	
	2006-10-23	2.3	Westeremden	3	
			‘t Zand 1	2	
	2006-04-26	2.3	Hoeksmeer	2	

Magnitude in M_L
Delta = epicentral distance in kilometres

4.2 Results

We provide two series of acceleration records.

a. Estimated horizontal and vertical acceleration time series (12 time series) for a magnitude M_L = 4.0 (Appendix figures A1-A3)
b. Observed horizontal and vertical acceleration time series (12 time series) for $2.3 \leq M_L \leq 2.5$ (Appendix figures A4 – A6)

The accelerations are plotted in the appendix (A1-A6) and delivered together with the electronic version of this report on the CDROM in ASCII format and appropriate explanation of the format.

The M_L = 4.0 accelerations are derived from the observed M_L = 3.5 event on 8 August 2006 (Table 1a) with an appropriate scaling. The rupture surface will not increase significantly and we assume no significant change in the rupture process. The consequence is that the source function for an M_L = 4.0 event may be less then 10% longer then the source time function for an M_L = 3.5 event. From some simple modelling experiments we concluded then that we do not expect significant frequency changes if we extrapolate from M_L = 3.5 to M_L = 4.0. However, other simple modelling calibration experiments show that we may well observe amplitude uncertainties in the order of a factor 2-4 (figure 4). These variations are mainly due to the shallow depth and consequently the small hypocentral distances we need to consider. The source radiation pattern has a significant influence, while the attenuation, imbedded in the Green’s function, has significantly less influence.

The observed accelerations for the events with magnitudes in the range of $2.3 \leq M_L \leq 2.5$ (Table 1c) are straight forward, but illustrate also the significant variations in the source radiation pattern. An extreme example of this influence of the source is shown in figure 35 in Van Eck et al. (2004). Also here similar uncertainty factors of around 2-4 are reasonable.

4.3 Site effect considerations

The observed accelerations are recorded on the surface and, consequently, they include a local site effect. None of the accelerometers are situated in the free field. In most cases they are situated on the ground or cellar floor of small buildings. Currently, we have not yet explored in detail the effect of these locations, but from preliminary experiments we expect them to be minor.

4.4 Instrumental corrections

The instrument response is flat for accelerations between 0.3 and 30 Hz (Dost and Haak, 2002). Therefore, no instrumental corrections have been applied beyond the amplification. All amplitudes are given in milli g.

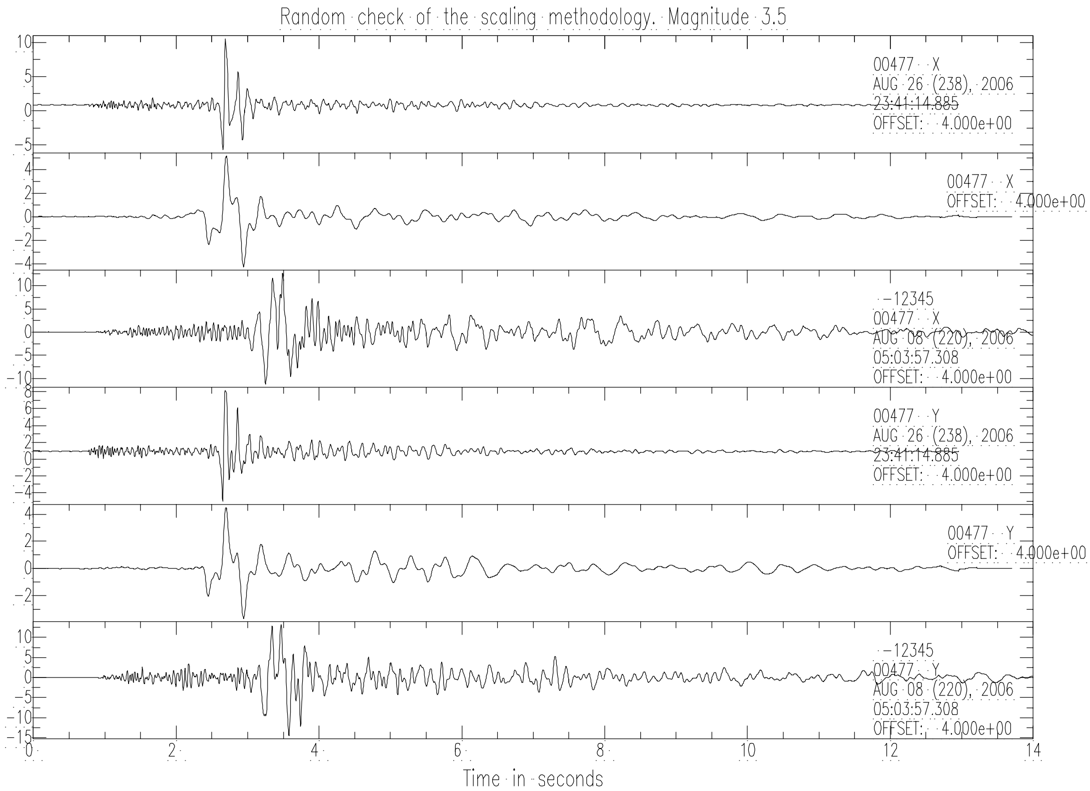

Figure 4. Random check of the modelling approach for 2 horizontal components. Given a M_L = 2.3 event and reconstruct an M_L = 3.5 event. The event epicentre locations are about 3 km apart and differ therefore most probably in source mechanism and consequently, source radiation pattern. From top to bottom; M_L = 2.3 event N-S motion, modelled M_L = 3.5 event, observed acceleration N-S motion, M_L = 2.3 event E-W motion, modelled M_L = 3.5 event, observed acceleration E-W motion. In these cases the amplitudes are underestimated by a factor 2 – 4. We did not consider the high frequency part of the source function in this modelling approach. Amplitudes are in milli g.

5. Source and radiation pattern

Seismicity in the Groningen Field is concentrated near existing faults on top of the gas reservoirs at a depth of 3 km. These faults are possibly re-activated. If the characteristics of these faults (strike, dip and rake) are known, we are able to calculate the amplitude effects at the surface resulting from a movement along these faults by means of a forward modelling. From our experience we believe that this source effect is dominant over any site-effect, but as we do not know the source mechanism in advance its effect remains unpredictable.

From seismic surveys we know that these faults are mainly steeply dipping normal faults. However, the Groningen field is a complex geological structure, where normal faults change their strike and dip over short distances. Also, the dip of these faults is not very well known, except for the fact that they are steep (60-90 degrees). In 2006 a M_L=3.5 earthquake did occur in the central part of the Groningen field, which was recorded by 4 accelerometers at close distances. This enabled us to compare fault modelling results with actual measurements. Moreover, two smaller events did occur in the same month, close to the main event, suggesting a strike of the fault of approximately 310 degrees. From geological maps (TNO-NITG) we identified a possible candidate fault dipping to the north-east.

In order to demonstrate the effects of a change in dip of the normal fault, we calculated the amplitudes of a source at 3 km depth, strike 310 degrees, rake 270 degrees (no lateral movement) and a dip of 90 degrees (vertical) and 70 degrees (20 degrees with the vertical). Modelling gives displacement at the surface, which is translated into velocity by assuming a dominant frequency of 3 Hz, measured from acceleration records close to the recent M_L=3.5 event.

The effect of a small change in fault dip of 20 degrees creates a significant directivity effect, showing for this north-east dipping example a strong effect to the south-west (figure 5). However, this directivity effect is limited to a region of 6-8 km from the source for a M_L=3.5 event and for a M_L=4.0 event an estimated 10-12 km region from the source is effected. Comparison with measured accelerations for the M=3.5 event shows larger velocities to the south-west. Also, damage reports from this events show a concentration to the south-west of the epicentre. Both observations are in agreement with our modelling.

In this model study it shows that for this specific case the source radiation effect from the currently most active faults about 10-15 km to the south-west of the Eemshaven area, would be limited. However, this model study also shows that we may expect a significant source effect from local fault segments close to the Eemshaven area. Up to now these faults show not much activity.

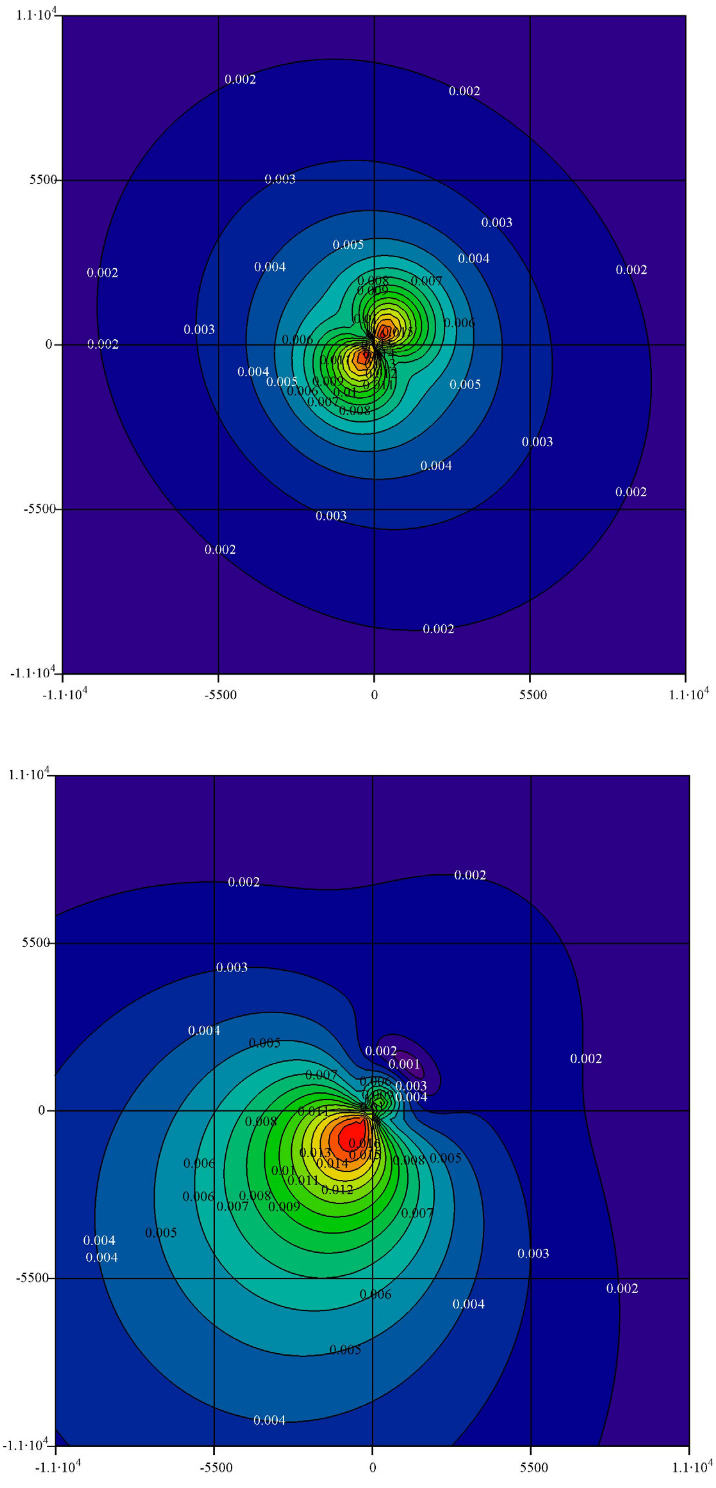

Figure 5. Fault modelling results illustrating the expected large S-wave amplitude variations due to two different source mechanisms for the same magnitude earthquake. X- and Y-axes show distance in meters with respect to the epicentre (0,0). Contours show velocity in m/s, resulting from a M_{L}=3.5 earthquake at 3 km depth. A normal fault with a 90 degrees dip (top) is compared to a 70 degrees dipping fault (bottom), both at strike 310 and rake 270 degrees.

6. Conclusions and discussion

We have provided 24 relevant ground accelerations for dynamical modelling. These accelerations are conservatively estimated to occur with an annual probability of 0.6 for earthquakes $M_L \geq 2.3$ and with an annual probability of about 0.001 for earthquakes with $M_L \geq 4.0$. For the small magnitude events we have records up to distances of 3 km. For the larger magnitude events we have records for distances up to 9 km.

The accelerations are characterized by small short pulses. The form and amplitude of those pulses may depend significantly on the source radiation pattern in relation to the source-site path. Observations have shown that within 6-8 km distance this can give rise to significant uncertainties very well ranging in between a factor 2 – 4 or, closer to the epicentre, more. A more detailed discussion of the uncertainties can be found in van Eck et al (2006).

7. References

- Aki, K. and P.G. Richards, 1980. *Quantitative Seismology*, Freeman and Co., New York, 932 pp.
- De Crook, Th., H.W. Haak and B. Dost, 1998. Seismisch risico in Noord-Nederland. KNMI Technisch Rapport TR-168, 30pp.
- Dost, B. and H.W. Haak, 2002. A comprehensive description of the KNMI seismological instrumentation. Technical Report TR-245, 60 pp.
- Haak, H.W., B. Dost and F.H. Goutbeek, 2001. Seismische analyse van de aardbevingen bij Alkmaar op 9 en 10 september en Bergen aan Zee op 10 oktober 2001. KNMI Report TR-239. 24pp.
- Logan, J.M., N.G. Higgs and J.W. Rudnicki, 1997. Seismicity risk assessment of e possible gas storage project in the Bergermeer field, Bergen concession. Report to BP. 20 pp. (confidential)
- Van Eck, T. F.H. Goutbeek, H.W. Haak and B. Dost, 2004. Seismic hazard due to small shallow induced earthquakes. Report KNMI, WR 2004-01, 52 pp.
- Van Eck T., F.H. Goutbeek, H.W. Haak and B. Dost, 2006. Seismic hazard due to small-magnitude, shallow-source induced earthquakes in the Netherlands. *Engineering Geology*, **87**, 105-121.

Appendix A. Acceleration time series

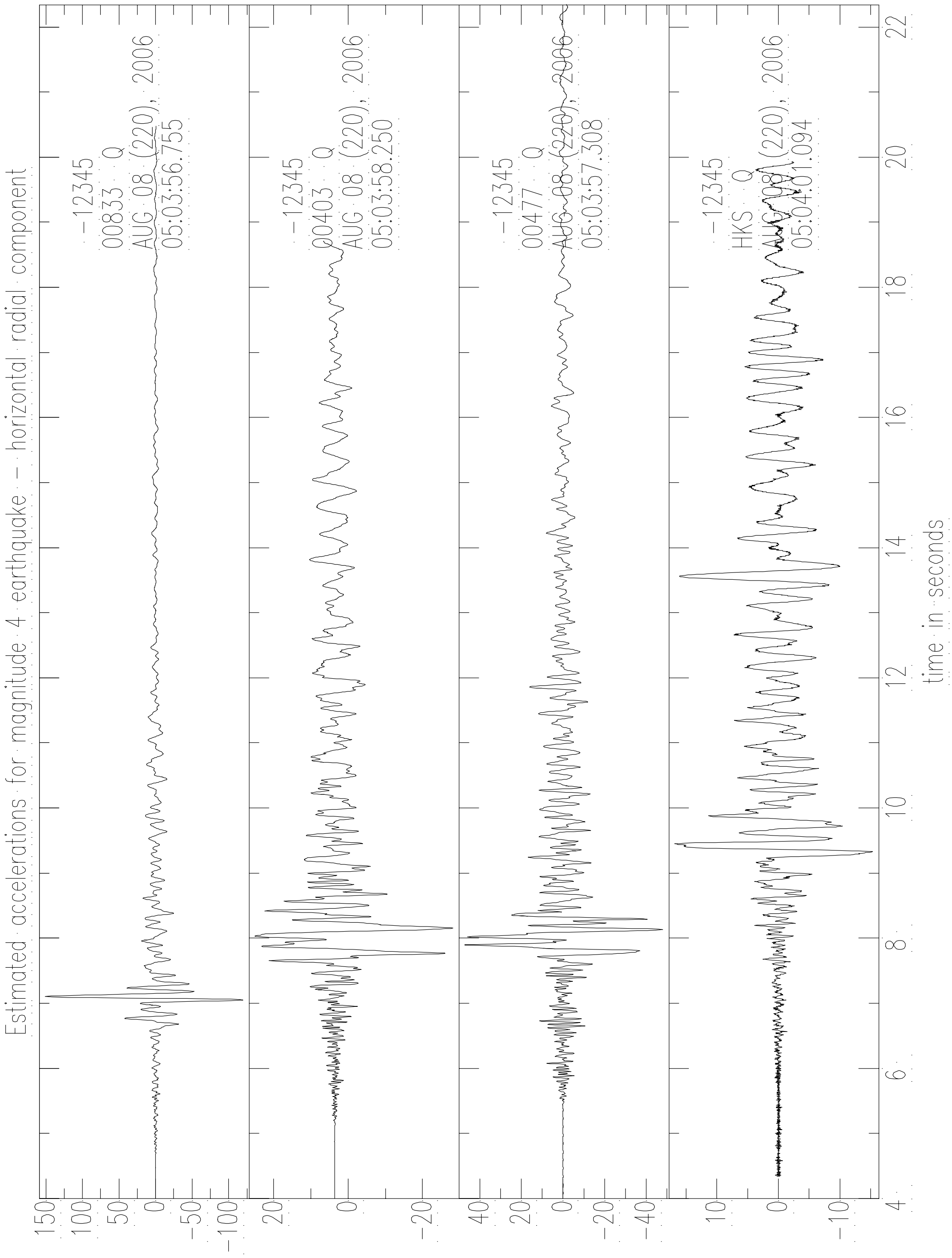

Figure A1. Estimated horizontal (radial directions) acceleration time series for a magnitude M_L = 4.0 earthquake (from left to right) at respectively 3, 4, 6 and 9 kilometres epicentral distance. The amplitudes are in milli g. [Filenames: acc-mag4-3km.r, acc-mag4-4km.r, acc-mag4-6km.r, acc-mag4-9km.r]

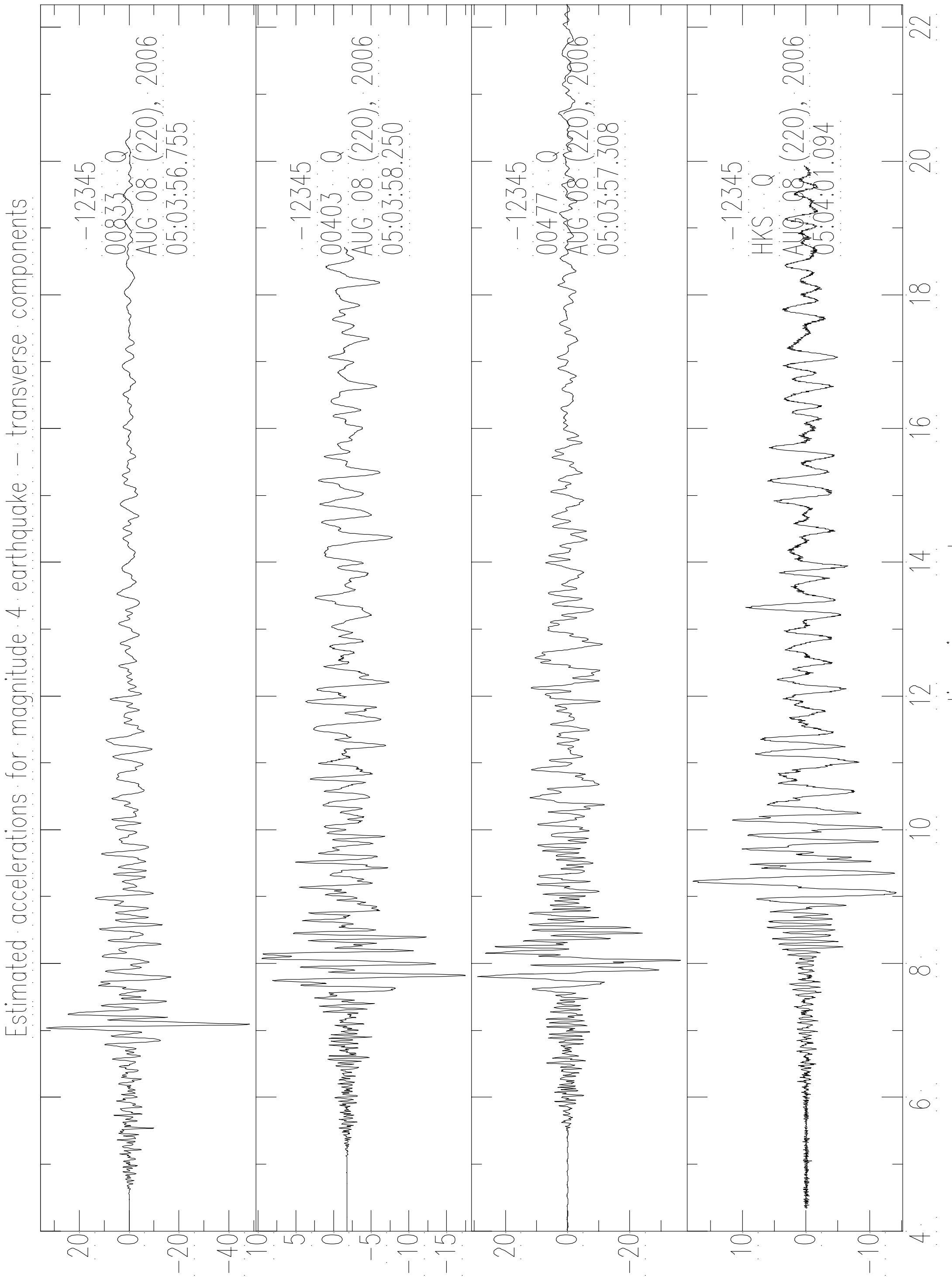

Figure A2. Estimated horizontal (transverse directions) acceleration time series for a magnitude M_L = 4.0 earthquake (from left to right) at respectively 3, 4, 6 and 9 kilometres epicentral distance. The amplitudes are in milli g. [Filenames: acc-mag4-3km.t, acc-mag4-4km.t, acc-mag4-6km.t, acc-mag4-9km.t]

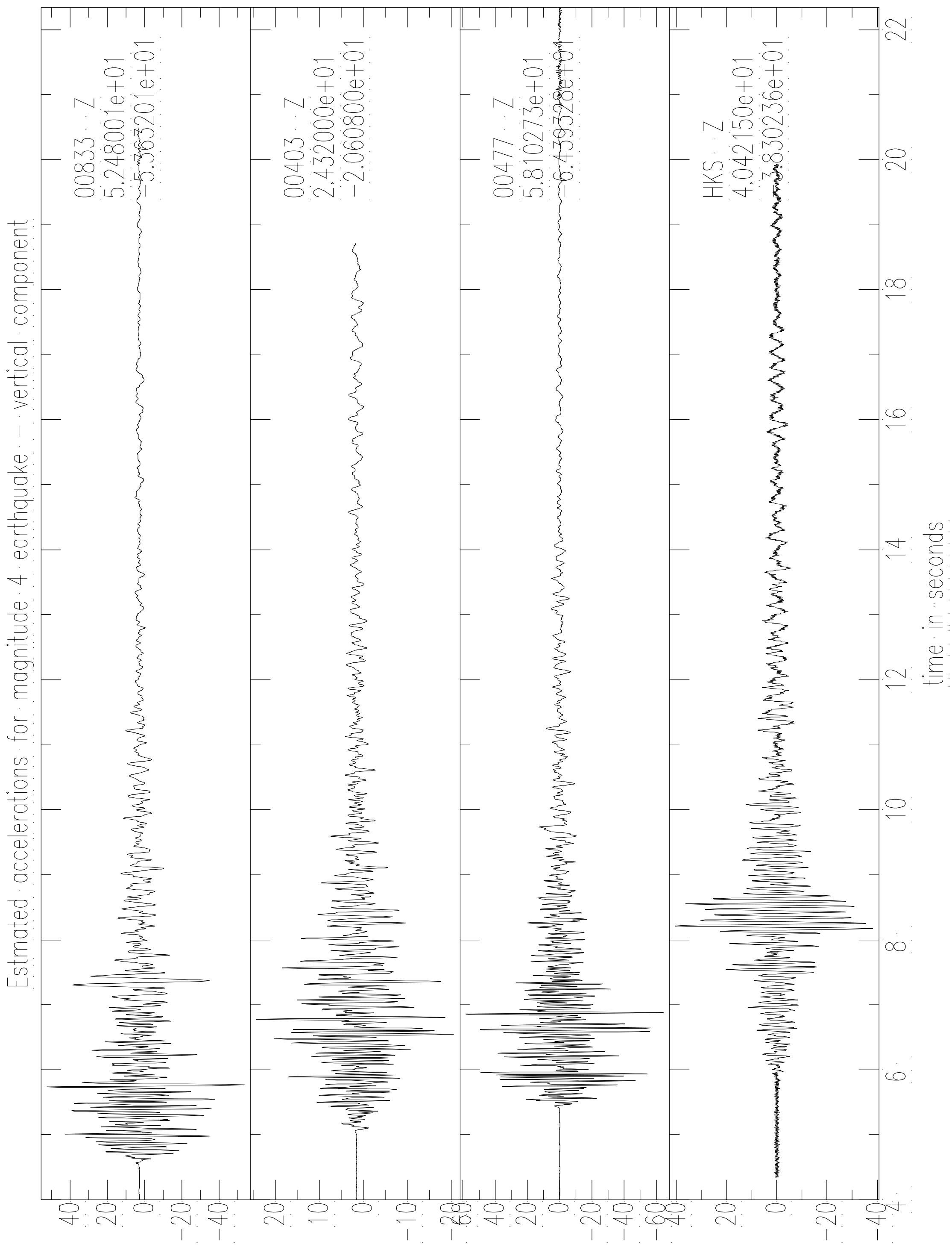

Figure A3. Estimated vertical acceleration time series for a magnitude $M_L = 4.0$ earthquake (from left to right) at respectively 3, 4, 6 and 9 kilometres epicentral distance. The amplitudes are in milli g. [Filenames: acc-mag4-3km-z, acc-mag4-4km-z, acc-mag4-6km-z, acc-mag4-9km-z]

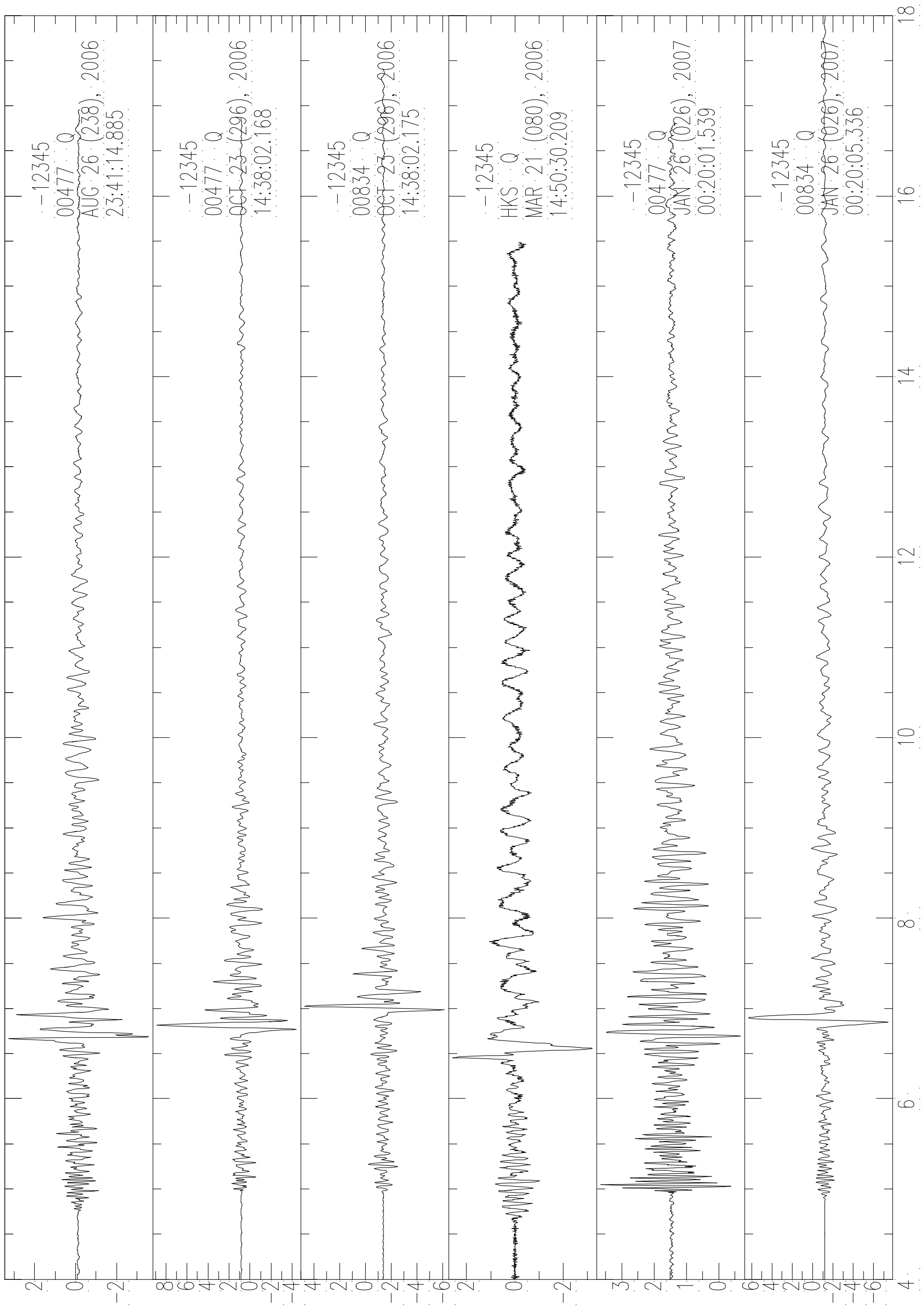

Figure A4. Horizontal (radial direction) observed acceleration time series for a magnitude distance combination (M_L , R in km) of (2.3, 4), (2.3, 1.8), (2.3, 3.1), (2.4, 2.3) and (2.5, 1.3) from left to right respectively. The amplitudes are in milli g. [Filenames: 060826.r; 061023a.r, 061023b.r, 060321.r, 070126a.r, 070126b.r]

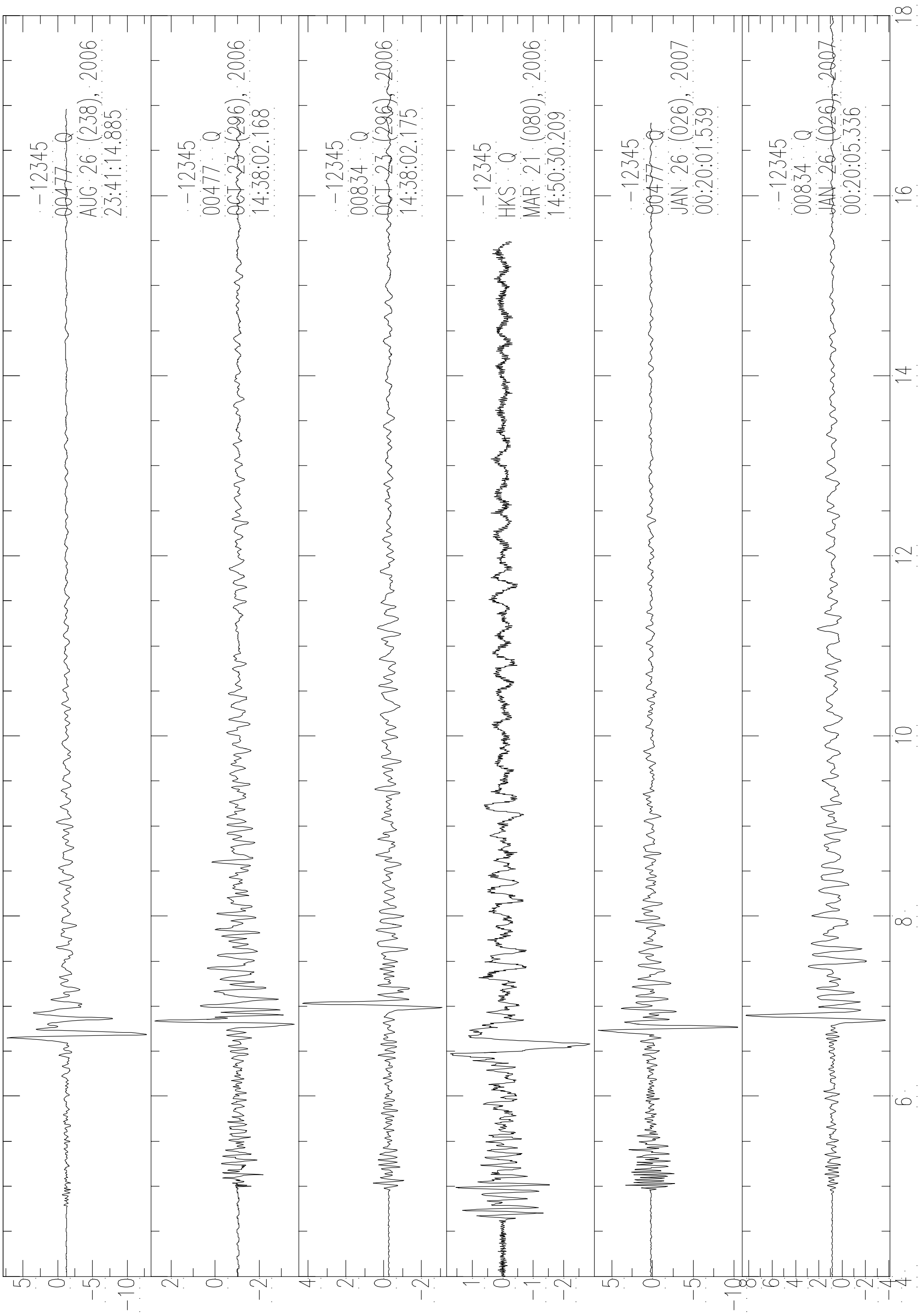

Figure A5. Horizontal (transverse direction) observed acceleration time series for a magnitude distance combination (M_L , R in km) of (2.3, 4), (2.3, 1.8), (2.3, 3.1), (2.4, 2.3) and (2.5, 1.3) from left to right respectively. The amplitudes are in milli g. [Filenames: 060826.t; 061023a.t, 061023b.t, 060321.t, 070126a.t, 070126b.t]

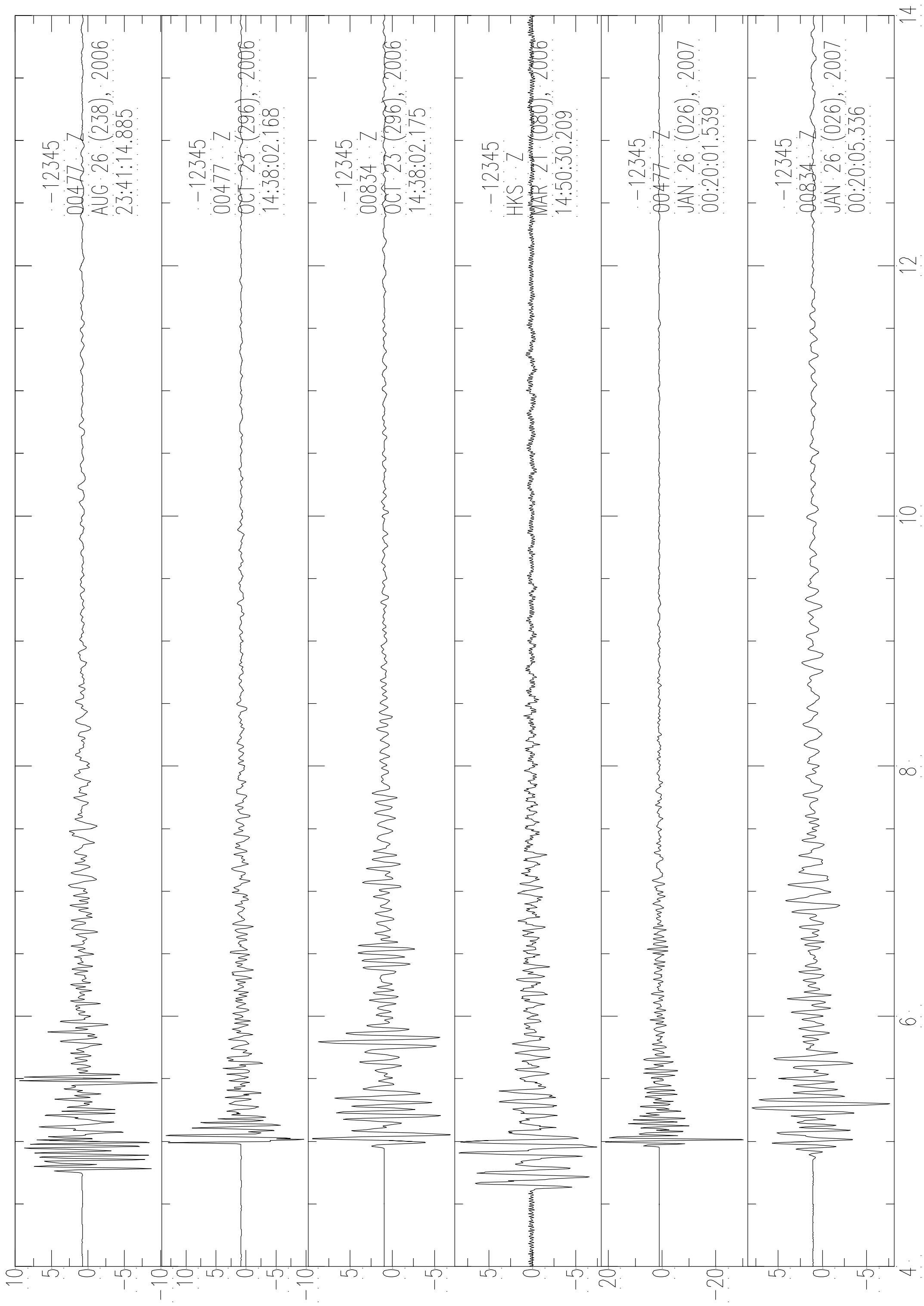

Figure A6. Vertical observed acceleration time series for a magnitude distance combination (M_L , R in km) of (2.3, 4), (2.3, 1.8), (2.3, 3.1), (2.4, 2.3) and (2.5, 1.3) from left to right respectively. The amplitudes are in milli g. [Filenames: 060826-z; 061023a-z, 061023b-z, 060321-z, 070126a-z, 070126b-z]